



# OPEN Exploring the anti-inflammatory effects of genistein in an in vitro lipopolysaccharide-induced macrophage model

Cristina Remirez de Ganuza<sup>1,2,3</sup>✉, Sonia López<sup>1,2</sup> & Gracia Mendoza<sup>3</sup>

Inflammation plays a central role in the onset and progression of numerous diseases, and macrophages are key regulators of this process through their polarization toward pro- or anti-inflammatory phenotypes. Natural bioactive compounds have emerged as promising candidates to modulate inflammatory responses. Amongst these, genistein, a soybean-derived isoflavone, was selected due to its reported anti-inflammatory and antioxidant profile across different cell types. In this study, we evaluated the effects of genistein in a lipopolysaccharide (LPS)-induced macrophage model to investigate its cellular and molecular mechanisms of action. Genistein treatment at subcytotoxic concentration preserved cell viability, did not induce apoptosis or cell cycle arrest, and reduced oxidative stress. In LPS-stimulated macrophages, treatment with 5 µg/mL genistein significantly decreased nitric oxide production and downregulated pro-inflammatory markers while upregulating an anti-inflammatory mediator, thus reverting macrophage polarization to an anti-inflammatory phenotype. Protein analyses confirmed reduced expression of iNOS and cytokines such as IL-6 and TNF-α. Furthermore, genistein restored cell morphology and inhibited NF-κB p65 nuclear translocation, indicating its capacity to counteract LPS-driven pro-inflammatory signalling. These findings support the role of genistein in modulating macrophage polarization and inflammatory responses, highlighting its therapeutic potential for the management of acute and chronic inflammation-related disorders.

**Keywords** Genistein, Macrophages, Inflammation, NF-κB signalling, Cytokine regulation, LPS

Inflammation is recognized as key factor in the initiation and progression of several diseases. Its role is essential as first response against external and internal stimuli which can contribute to cell damage. The activation of inflammatory signaling pathways tries to repair the potential injury through the elimination of the harmful agent and the damaged cells as well as boosting the regeneration mechanisms<sup>1</sup>. However, the dysregulation or chronification of inflammation may result in the development of different pathologies, such as cardiovascular diseases, cancer, metabolic diseases or osteoarticular diseases.

The inflammatory response involves the activation of organized signaling pathways resulting in the recruitment of inflammatory cells from other tissues, mainly the blood, and the regulation of resident inflammation mediator levels. The target tissue and the initiator stimulus are determinant in the progression of the inflammatory process though all of them share the same molecular events<sup>2,3</sup>. The main molecular hallmarks in inflammation are the activation of key intracellular signaling pathways such as the nuclear factor kappa-B (NF-κB) pathway, the mitogen-activated protein kinase (MAPK) pathway or the activator of transcription (STAT) pathway, among others<sup>3</sup>.

Macrophages play a pivotal role in the activation of these inflammatory signaling pathways through the expression on their surface of toll-like receptors (TLRs) and the activation of T cells mediated by major histocompatibility II (MHC II) molecules. This activation triggers different signaling pathways that result in the polarization of naïve macrophages (M0) into their proinflammatory (M1) or anti-inflammatory phenotype (M2)<sup>4-7</sup>. M1 phenotype is characterized by the production and secretion of proinflammatory cytokines such as

<sup>1</sup>Instituto de Nanociencia y Materiales de Aragón (INMA), CSIC-Universidad de Zaragoza, Zaragoza 50009, Spain.

<sup>2</sup>Department of Chemical and Environmental Engineering, University of Zaragoza, Campus Río Ebro-Edificio I+D, C/Poeta Mariano Esquillor S/N, Zaragoza 50018, Spain. <sup>3</sup>Aragon Health Research Institute (IIS Aragon), Zaragoza 50009, Spain. ✉email: 736848@unizar.es

tumor necrosis factor- $\alpha$  (TNF- $\alpha$ ), interleukin-1 beta (IL-1 $\beta$ ), and interleukin-6 (IL-6), while M2 phenotype can express anti-inflammatory markers, including arginase-1 (Arg-1) and interleukin 10 (IL-10), facilitating tissue repair<sup>8,9</sup>. However, the persistence in M1 phenotype may result in an imbalance of M1/M2 ratio, and thus, in the dysregulation of inflammation and tissue damage.

The involvement of this imbalance in severe pathologies such as cardiovascular diseases, cancer or autoimmune diseases, has sparked interest in the search of anti-inflammatory strategies, including those based on natural compounds. Different strategies are being developed to alleviate inflammatory diseases through the targeting of inflammatory signaling pathways, inflammasome or specific cytokines. These approaches are mediated by small molecule-inhibitors, diverse drugs or natural biologically active compounds which are able to diminish inflammation, and may therefore be useful in the treatment of inflammation-related diseases<sup>1,10</sup>.

Several natural biologically active compounds have shown promise in preventing or inhibiting acute and chronic inflammatory states involved in metabolic diseases, renal pathologies, cancer or osteoarticular diseases, by modulating key molecular targets<sup>11,12</sup>. Specifically, isoflavones have attracted increasing interest regarding their antioxidant and anti-inflammatory profile demonstrating their potential therapeutic effects. Genistein is a 4',5,7-trihydroxyisoflavone mainly found in soybeans and soy products which has been shown to regulate molecular mediators including TLR-4, cytokines (i.e. IL-1 $\beta$ , IL-6, TNF- $\alpha$ ), MAPK and NF- $\kappa$ B pathways, not only in vitro but also in preclinical studies<sup>13–17</sup>. Although other flavonoids exhibit potent and more selective anti-inflammatory effects, genistein is a pleiotropic molecule whose biological actions extend beyond its anti-inflammatory profile. As a phytoestrogen, genistein is able to interact with estrogen receptors (particularly ER $\beta$ ), modulating immune and metabolic pathways<sup>18</sup>. Genistein is also an inhibitor of several tyrosine kinases, contributing to its ability to regulate cell differentiation and proliferation<sup>18</sup>. In addition, it exerts antioxidant effects<sup>19</sup>, and influences epigenetic marks, including DNA methylation and histone acetylation, thereby regulating the expression of multiple target genes<sup>20</sup>.

This study aims to shed light on the cellular and molecular events involved in the treatment of lipopolysaccharide (LPS)-stimulated macrophages with the isoflavone genistein. Specifically, the anti-inflammatory effects and the potential inhibitory activity of genistein on cellular and molecular markers were analyzed to evaluate its potential as novel therapeutic strategy in the treatment of acute and chronic inflammatory diseases.

## Results and discussion

### Cellular effects of genistein treatment on macrophages

J774 murine macrophages were treated with genistein (1–50  $\mu$ g/mL) for 24 h to assess the biological effects of the tested isoflavone regarding cell viability, cell cycle and apoptosis. The evaluation of cell viability by the Blue Cell Viability Assay showed that 5  $\mu$ g/mL corresponded to the highest concentration that did not induce cytotoxicity according to ISO 10993-5 (< 30% viability reduction) (Fig. 1a)<sup>21</sup>. The selected concentration lies within the range commonly achieved after high-dose dietary genistein intake or supplementation (1–5  $\mu$ M) reported in human pharmacokinetic studies<sup>22–24</sup>.

Flow cytometry assays were developed to evaluate the effects of genistein in cell cycle and apoptosis. Figure 1b demonstrates that macrophages treatment with the subcytotoxic concentration (5  $\mu$ g/mL) did not involve significant changes, only a slight increase in G1 (5.93%) with the subsequent decrease in G2 (2.56%). Conversely, cell treatment with genistein yielded a slight increase in apoptosis (early + late) being lower than 10% with the concomitant reduction in viability. The slight increase in apoptosis likely reflects a minimal cellular stress response rather than a relevant cytotoxic effect. This is supported by the fact that overall viability remained high and the cell-cycle profile was unchanged. Given the small magnitude of the effect (< 10%), this increase is unlikely to compromise macrophage homeostasis under the conditions tested.

These results are in accordance with previous studies in other murine macrophage cell lines in which cell treatment with genistein for 24 h and at concentrations similar to that used in our studies ( $\leq$  25  $\mu$ M) yielded no effects in cell biological status<sup>17,25</sup>. Thus, 5  $\mu$ g/mL represents a biologically active but non-toxic dose that allowed mechanistic evaluation without compromising cell viability.

On the other hand, cell oxidative status after genistein treatment was evaluated by means of the measurement of mitochondrial membrane potential, reactive oxygen species (ROS) and proteasome 20 S activity (Fig. 2). Cell oxidative status is essential to maintain cell function and viability. Thus, cell integrity after treatment is crucial for the intended biomedical application of genistein.

After treatment of J774 macrophages with genistein for 24 h, the mitochondrial membrane potential was increased around 15% (Fig. 2A) while ROS production was significantly decreased when cells were also induced by H<sub>2</sub>O<sub>2</sub> (Fig. 2B), demonstrating the antioxidant profile of genistein to macrophages. Several studies have demonstrated the ability of genistein to suppress ROS generation across a wide range of cellular systems and oxidative stimuli<sup>26–31</sup>. These findings indicate that the reduction in ROS observed in our macrophage model is consistent with the broad and stimuli-independent antioxidant activity described for genistein.

Moreover, the activity of proteasome 20 S was slightly decreased (Fig. 2C). The implication of the 20 S subunit of proteasome in the activation of NF- $\kappa$ B signalling pathway is highly relevant for the inflammatory status of cells<sup>32</sup>. The ubiquitin-proteasome system is the primary pathway for protein degradation in eukaryotic cells<sup>32</sup>. Proteasomes are enzymatic complexes that degrade damaged or unneeded proteins. The 26 S proteasome consist of the 20 S core, responsible for proteolysis, and the 19 S regulatory particle. The 20 S proteasome plays a central role in controlling protein turnover and regulating key signalling pathways, including NF- $\kappa$ B<sup>33</sup>. Under physiological conditions, NF- $\kappa$ B is sequestered in the cytoplasm by its inhibitory protein I $\kappa$ B, preventing it from activating gene transcription<sup>33</sup>. Upon certain stimuli, such as inflammation or cellular stress, I $\kappa$ B is phosphorylated and degraded by 20 S, which allows NF- $\kappa$ B to translocate to the nucleus and induce the transcription of genes involved in inflammation, cell survival and immune responses. Inhibition of 20 S activity

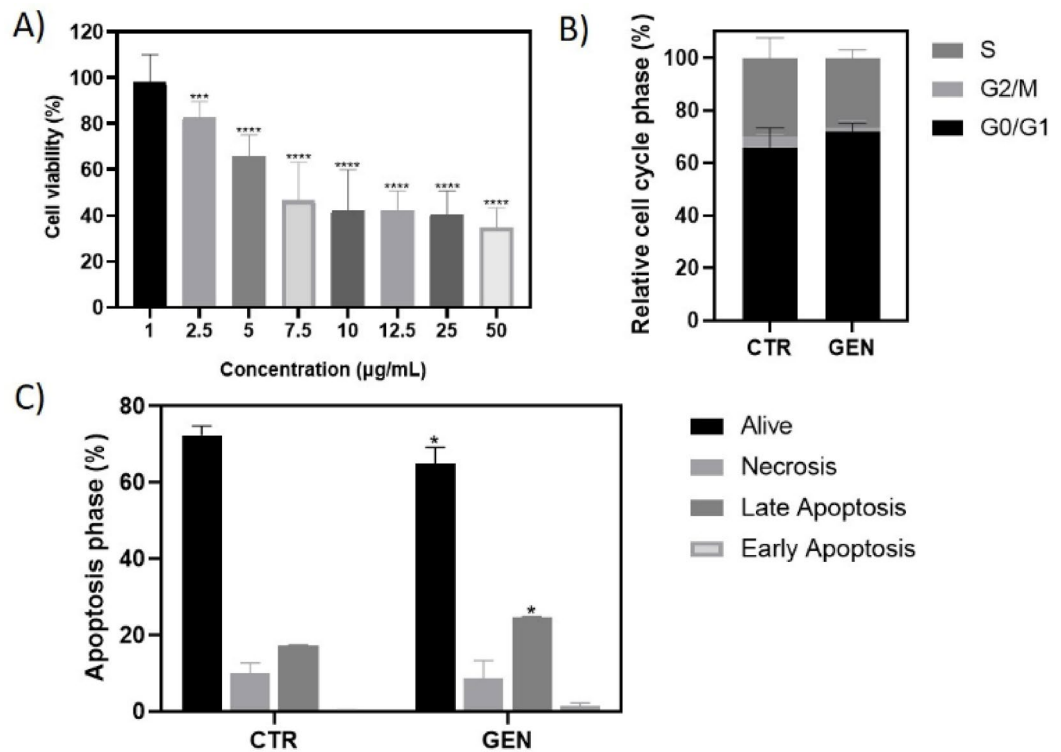


**Fig. 1.** Evaluation of macrophage viability, cell cycle and apoptosis. **(A)** Macrophage viability after incubation for 24 h with genistein (1–50 µg/mL). **(B)** Relative cell cycle phases in macrophages after 24 h incubation in absence (CTR; control sample) or presence of genistein (5 µg/mL). **(C)** Percentage of cell apoptosis by flow cytometry after 24 h incubation in absence (CTR; control sample) or presence of genistein (5 µg/mL). Data are represented as mean ± standard deviation (SD) obtained from at least three independent biological experiments, performed in triplicate (\* $p \leq 0.05$ ; \*\*\* $p \leq 0.001$ ; \*\*\*\* $p \leq 0.0001$  vs. control).

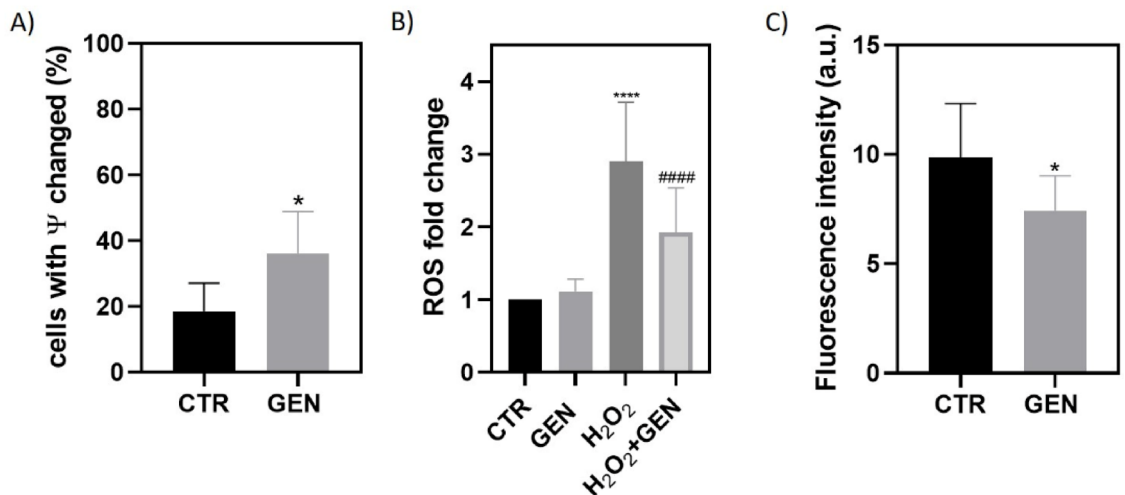


**Fig. 2.** Role of genistein in oxidative stress in macrophages after 24 h incubation with genistein (5 µg/mL). **(A)** Analysis of mitochondrial membrane potential. **(B)** Measurement of ROS production on macrophages in absence (CTR; control sample) or presence of H<sub>2</sub>O<sub>2</sub> (80 mM for 20 min). **(C)** Proteasome 20 S activity in macrophages. Data are represented as mean ± SD obtained from at least three independent biological experiments, performed in triplicate (\* $p \leq 0.05$ , \*\*\*\* $p \leq 0.0001$  vs. control; #### $p \leq 0.0001$  vs. H<sub>2</sub>O<sub>2</sub>).

prevents I $\kappa$ B degradation, retaining NF- $\kappa$ B in the cytoplasm. In this study, genistein significantly reduced 20 S proteasome activity, suggesting a mechanism for downregulating NF- $\kappa$ B signalling.

These results, together with those depicted in Fig. 1, demonstrated that genistein treatment did not involve detrimental effects in macrophages as it has been widely shown for other cell lines, mainly tumour cells<sup>34,35</sup>. Moreover, genistein exerts a consistent inhibitory effect on ROS generation across different cell types, which likely contributes to its anti-inflammatory activity<sup>26,30,31</sup> and additionally reduces the activity of the 20 S proteasomal subunit, potentially limiting NF- $\kappa$ B activation and downstream inflammatory responses.

### Molecular effects of inflammation induction mediated by LPS and genistein treatment on macrophages

The molecular anti-inflammatory effects of genistein were studied in LPS-stimulated macrophages following a pre-treatment approach and a post-treatment approach, as detailed below, through the evaluation of nitric oxide (NO) production, gene expression of pro- and anti-inflammatory markers by RT-qPCR, Western Blot, ELISA assays, and the qualitative evaluation of changes in cell morphology and NF- $\kappa$ B translocation by confocal microscopy. While the inhibitory effects of genistein on NO release and iNOS expression are well documented, as well as its anti-inflammatory potential, here we use a physiologically relevant sub-cytotoxic concentration (much lower than those usually tested), and in the direct comparison of pre and post-treatment approaches, providing insights into both preventive and restorative anti-inflammatory actions.

NO production after macrophage induction with LPS was significantly increased in J774 macrophages compared to the control sample (not treated cells) (Figs. 3A and 4A). The treatment of cells with genistein involved a significant reduction in NO production ( $\approx$  35% in the pre-treatment strategy and  $\approx$  20% in the post-treatment strategy) demonstrating the potential antioxidant and anti-inflammatory capacity of genistein. Comparable reduction in LPS-induced NO production has been reported in both RAW 264.7 and J774 macrophages treated with genistein, although the magnitude of the response differed depending on the concentration of genistein, the timing of exposure and, importantly, the dose and source of LPS used<sup>36–40</sup>. In this context, Hämäläinen et al.<sup>40</sup> reported that the treatment of J774 macrophages at the same LPS concentration used in our assay (100 ng/mL) and 10  $\mu$ M genistein (vs. 18,5  $\mu$ M) for 24 h, resulted in an  $11.6 \pm 2.4\%$  inhibition relative to LPS-treated cells, results that are consistent with those observed in the present study. However, it is worth mentioning that even if the same concentration of LPS was used, its molecular effects can vary depending on its origin and structural differences, affecting immune response and signalling pathways<sup>41,42</sup>. Overall, our findings fall within the range of previously reported effects and support the capacity of genistein to attenuate NO production under inflammatory challenge.

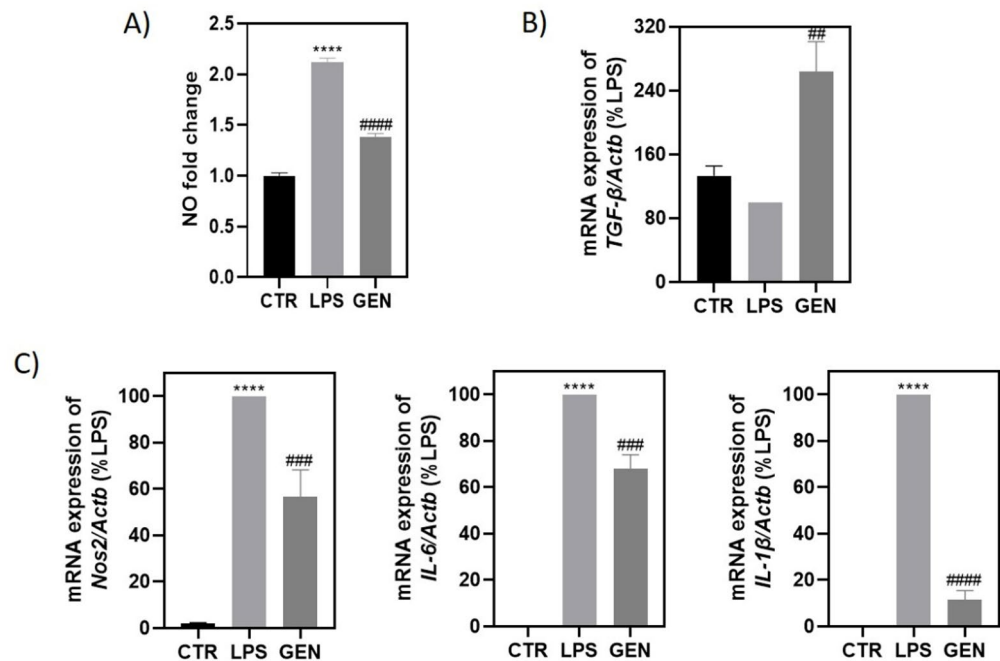


**Fig. 3.** Nitric oxide (NO) production and gene expression of pro- and anti-inflammatory markers in J774 murine macrophages by quantitative PCR (qPCR) in the pre-treatment strategy. **(A)** NO production. **(B)** Expression levels of the anti-inflammatory marker TGF- $\beta$ . **(C)** Expression levels of the pro-inflammatory markers Nos2, IL-6 and IL-1 $\beta$ . The level of the target mRNA was normalized to that expressed by *Actb* with gene expression in LPS-treated cells arbitrarily set to 100%. CTR, no treatment; LPS, lipopolysaccharide; GEN, genistein. Data are represented as mean  $\pm$  SD obtained from at least three independent biological experiments, performed in triplicate. (\*\*\*\* $p \leq 0.0001$  vs. control; \* $p \leq 0.1$ , \*\* $p \leq 0.01$ , \*\*\* $p \leq 0.001$ , \*\*\*\* $p \leq 0.0001$  vs. LPS).

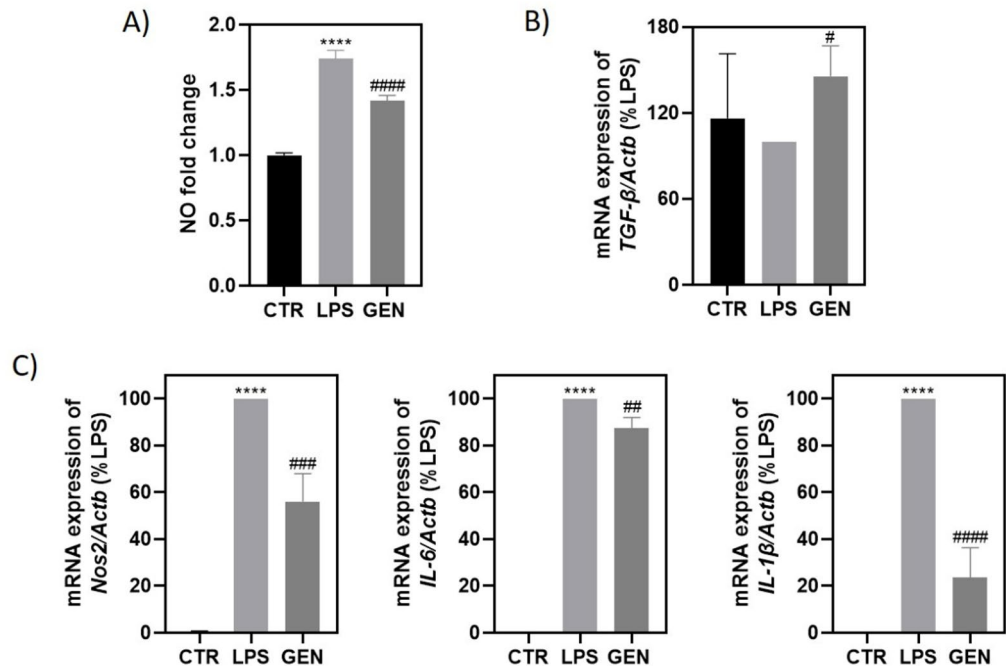


**Fig. 4.** Nitric oxide (NO) production and gene expression of pro- and anti-inflammatory markers in J774 murine macrophages by quantitative PCR (qPCR) in the post-treatment strategy. **(A)** NO production. **(B)** Expression levels of the anti-inflammatory marker TGF- $\beta$ . **(C)** Expression levels of the pro-inflammatory markers Nos2, IL-6 and IL-1 $\beta$ . The level of the target mRNA was normalized to that expressed by *Actb* with gene expression in LPS-treated cells arbitrarily set to 100%. CTR, no treatment; LPS, lipopolysaccharide; GEN, genistein. Data are represented as mean  $\pm$  standard deviation (SD) obtained from at least three independent biological experiments, performed in triplicate (\*\*\*\* $p \leq 0.0001$  vs. control; # $p \leq 0.1$ , ## $p \leq 0.01$ , ### $p \leq 0.001$ , #### $p \leq 0.0001$  vs. LPS).

Further studies, regarding the expression of characteristic pro-inflammatory markers (Nos2, IL-6 and IL-1 $\beta$ ) and the anti-inflammatory marker TGF- $\beta$ , confirmed these results highlighting the significant decrease in pro-inflammatory markers expression while the anti-inflammatory marker expression was significantly increased (Figs. 3B and C and 4B and C). Thus, the treatment with genistein resulted in the shift of macrophage polarization towards an anti-inflammatory phenotype. It should be noted that IL-1 $\beta$  was the most downregulated gene in both approaches (80–90% expression reduction) suggesting the involvement of genistein in the inhibition of the NF- $\kappa$ B signalling pathway. Consistent with our results, several studies have shown that genistein reduces the expression of key pro-inflammatory cytokines such as IL-6, TNF- $\alpha$  and iNOS in LPS-stimulated macrophages<sup>17,37,38,40</sup>. This inhibitory effect has been reported across a wide range of genistein concentrations and inflammatory conditions in both RAW 264.7 and J774 cells, reflecting its robust anti-inflammatory action despite differences in experimental design. Although macrophages are the primary producers of proinflammatory cytokines that drive the amplification of the inflammatory response<sup>26</sup>, the suppressive effect of genistein on pro-inflammatory cytokine gene expression has also been demonstrated in other cell lines<sup>43,44</sup>.

Other authors also demonstrated the significant increase in the expression of the anti-inflammatory markers AhR, IL-10 and Arg-1 in RAW 264.7 macrophages stimulated with IL-4 (20 ng/mL) and treated with genistein (25–200  $\mu$ M)<sup>16</sup>.

Protein expression was analysed by Western Blot and ELISA methodologies (Figs. 5 and S1). iNOS was overexpressed in LPS-induced macrophages in both strategies tested being significantly depleted by the addition of genistein (60–70%) (Fig. 5A and D), in accordance with the results obtained in the qPCR assays (Figs. 3 and 4). Other authors have also demonstrated the inhibitory effect of genistein on iNOS protein expression in LPS-activated macrophages. Studies in murine macrophages have consistently shown that genistein reduced iNOS levels in a dose-dependent manner, although the magnitude of inhibition differed depending on the concentration of genistein and the strength of the inflammatory stimulus<sup>37,38,40</sup>. While higher genistein doses and elevated LPS concentrations tend to produce more pronounced effects, even moderate concentration comparable to those in our work have been shown to attenuate iNOS expression.

ELISA assays (Fig. 5E and H) highlighted the significant depletion in the protein expression of the pro-inflammatory cytokines tested when cells were treated with genistein, being more remarkable for IL-6 expression (40–60% vs. 10–20% TNF- $\alpha$  expression). Ji et al.<sup>17</sup> pre-treated the same cell line with genistein (0.1–10  $\mu$ M) for 1 h followed by an incubation with LPS (1  $\mu$ g/mL) for 24 h, and obtained a significant and dose-dependently reduction of IL-6 and TNF- $\alpha$  production. Similarly, other authors have also reported a significant reduction in IL-6 production starting at 20  $\mu$ M genistein (vs. 18.5  $\mu$ M in our assays), when pre-treating for 30 min and incubating with LPS 10  $\mu$ g/mL for 24 h in RAW 264.7 cells<sup>37</sup>. Similar to what was observed with gene expression,

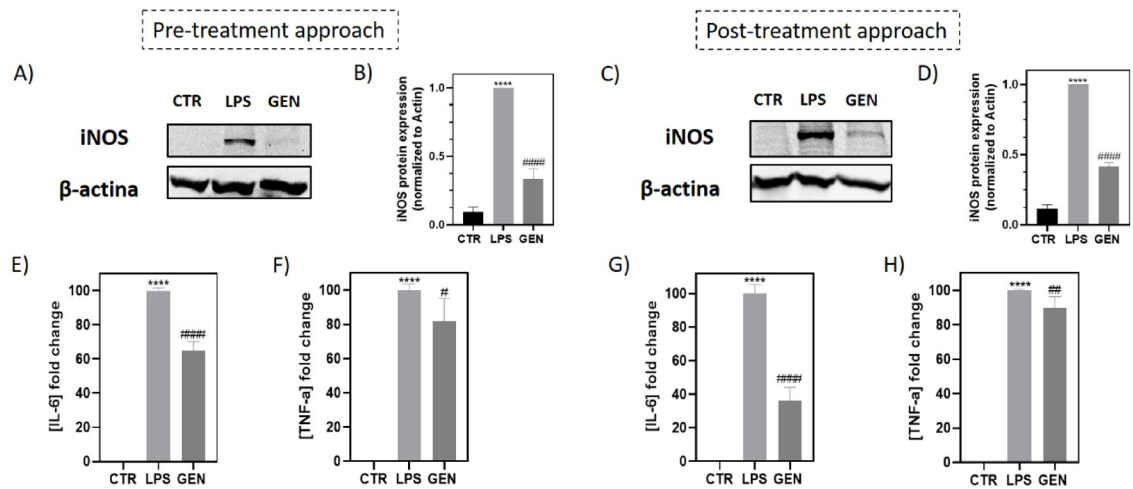


**Fig. 5.** Protein expression and quantitative evaluation in J774 murine macrophages. Western blot analysis of iNOS protein expression (A–D) and ELISA assays of the cytokines IL-6 and TNF- $\alpha$  (E–H), both in the pre-treatment and post-treatment approaches are depicted. Blots were cropped from different sections of the same gel and analyzed using Image J (full-length images are shown in Figure S1). Data are represented as mean  $\pm$  SD obtained from at least three independent biological experiments, performed in triplicate (\*\*\*\* $p \leq 0.0001$  vs. control; # $p \leq 0.1$ , ## $p \leq 0.01$ , ### $p \leq 0.0001$  vs. LPS).

the production of pro-inflammatory cytokines is also reduced among other cell lines as a consequence of genistein treatment<sup>26</sup>, which supports our results in macrophages.

LPS binding to receptors of the macrophage membrane leads to the activation of NF- $\kappa$ B signalling pathway and changes in cell morphology<sup>45</sup>. These effects in cell morphology were evaluated by confocal microscopy (Fig. 6). LPS induction involved remarkable changes in morphology where rounded cells became elongated and with lamellipodia (Fig. 6A and C). The treatment of macrophages with genistein, both in the pre- and post-treatment strategies, exerted the reversion of cell morphology to the control cells one, and a highly significant depletion of cell size to levels close to the control samples (not treated and not induced cells). Given the fact that genistein can modulate tyrosine kinase signalling, which directly regulate cytoskeletal dynamics, the morphological reversion observed may, at least in part, be mediated through this mechanism.

NF- $\kappa$ B p65 subunit is located in the cytosol of inactivated macrophages. I $\kappa$ B is its inhibitor and, in this state, it appears complexed to the p65 subunit. I $\kappa$ B phosphorylation by LPS or proinflammatory cytokines results in its ubiquitination and degradation and thus, the activated p65 subunit is released and translocated into the nucleus favouring the expression of target genes. The changes in the nuclear translocation of NF- $\kappa$ B p65 subunit were evaluated in LPS-stimulated macrophages pre-treated with genistein by confocal microscopy (Fig. 7). Cell induction with LPS resulted in the nuclear translocation of p65 subunit which was almost reverted when genistein was added, showing its expression predominantly in the cytoplasm. Accordingly, previous studies in LPS-induced RAW 264.7 macrophages pre-treated with 10  $\mu$ M genistein, in which the expression of the p65 subunit was tested by Western Blot, also showed the almost complete reversal of its expression to the control sample level after 24 h of treatment<sup>17</sup>. Similarly, incubation of J774 cells with LPS 100 ng/mL and 100  $\mu$ M genistein for 30 min inhibited the activation of NF- $\kappa$ B induced by LPS, also using Western Blot to detect the p65 subunit<sup>40</sup>. However, other authors did not find this reversion in RAW 264.7 macrophages by EMSA techniques after genistein pre-treatment (20  $\mu$ M) and LPS stimulation<sup>29</sup>. Therefore, genistein may be able to disrupt the nuclear translocation of NF- $\kappa$ B p65, confirming its anti-inflammatory capacity and the potential reversion of macrophages polarization. The effect of genistein on NF- $\kappa$ B inhibition has also been reported in other cells types<sup>26</sup>, thus confirming our results.

Given the pleiotropic nature of genistein, it is plausible that part of the anti-inflammatory effects described in this study involve pathways beyond NF- $\kappa$ B inhibition, such as modulation of MAPKs<sup>46</sup>, antioxidant responses<sup>19</sup> or tyrosine kinase-mediated signalling<sup>18</sup>.

Most studies evaluating genistein in macrophages have used higher concentrations (> 25  $\mu$ M) than ours, or focused on isolated endpoints. In this work, we examined a non-toxic, physiologically relevant concentration (5  $\mu$ g/mL), including pre/post-treatment approaches, and integrating oxidative, morphological and molecular markers. These extensive analyses allow a more realistic assessment of genistein's potential to modulate macrophage phenotype.

Despite its beneficial effects, genistein presents several limitations. Its pleiotropic nature and limited molecular specificity (compared to other flavonoids) may complicate mechanistic interpretation. Additionally, its weak estrogenic activity may raise considerations for certain biological models<sup>47</sup>. However, the concentrations required to elicit measurable effects in vitro are slightly higher than typical plasma levels, reflecting the limited bioavailability<sup>47</sup>. These aspects should be carefully considered when translating in vitro findings to the clinical practice.

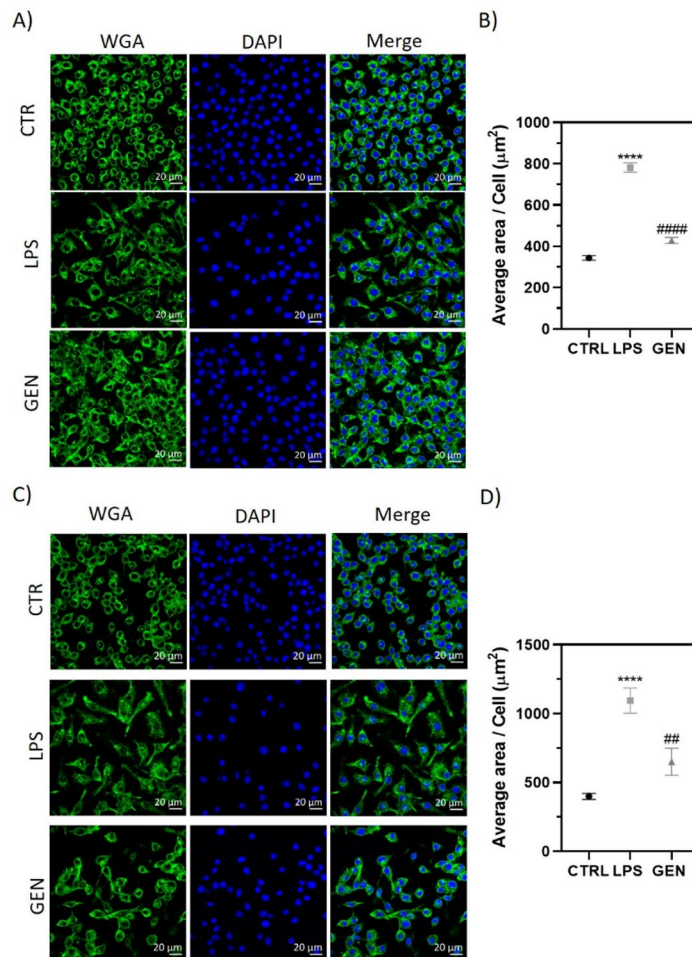


**Fig. 6.** Confocal microscopy images of J774 murine macrophages stained for cell membrane (green) and nuclei (blue). **(A)** Pre-treatment methodology. **(B)** Average area per cell calculated from the total area obtained in cell membrane and dividing it by the total number of events counted (nuclei) in the pre-treatment approach. **(C)** Post-treatment methodology. **(D)** Average area per cell calculated from the total area obtained in cell membrane and dividing it by the total number of events counted (nuclei) in the post-treatment approach. CTRL, no treatment; LPS, lipopolysaccharide; GEN, genistein. Data are represented as mean  $\pm$  SD obtained from at least three independent biological experiments, performed in triplicate. \*\*\*\* $p \leq 0.0001$  vs. control; ## $p \leq 0.01$ , #### $p \leq 0.0001$  vs. LPS.

## Materials and methods

### Materials

Genistein ( $\geq 98\%$  purity), Griess reagent and Lipopolysaccharide (LPS) from *Escherichia coli* O111:B4 were purchased from Sigma-Aldrich (Saint Louis, USA). Dimethyl sulfoxide (DMSO) was obtained from PanReac Applichem (Castellar del Valles, Spain). Phosphate-buffered saline (PBS), high-glucose Dulbecco's Modified Eagle Medium (DMEM w/stable glutamine) and antibiotic-antimycotic (60  $\mu\text{g}/\text{mL}$  penicillin, 100  $\mu\text{g}/\text{mL}$  streptomycin and 0.25  $\mu\text{g}/\text{mL}$  amphotericin B) were obtained from Biowest (Nuaille, France). Fetal Bovine Serum (FBS) was purchased from Gibco (Waltham, USA). TRIzol and wheat germ agglutinin Alexa Fluor™ 488 Conjugate were purchased from Invitrogen (Waltham, USA). PrimeScript™ RT Master Mix and PremixExTaq (ProbeqPCR) were obtained from Takara Bio (Shiga, Japan). iNOS antibody was purchased from Abcam (Cambridge, UK), GAPDH antibody from Bioss (Woburn, USA) and mouse anti-rabbit IgG-HRP sc-2357-CM secondary antibody was obtained from Santa Cruz Biotechnology Inc. (Dallas, USA).

### Cell culture and viability

J774A.1 macrophage cells (ATCC® TIB-67™) were cultured in DMEM supplemented with 10% FBS (v/v) and 1% antibiotic-antimycotic at 37 °C in a humidified atmosphere with 5% CO<sub>2</sub>.

The viability of cells was assessed using the Blue Cell Viability Assay (Abnova, Taipei, Taiwan). In brief, cells ( $2 \times 10^4$  cells/cm<sup>2</sup>) were seeded in 96-well plates and treated with genistein (1–50  $\mu\text{g}/\text{mL}$ ) dissolved in DMSO ( $\leq 0.25\%$  v/v) for 24 h at 37 °C. After treatment, the reagent was added to the cells to evaluate the viability following the manufacturer's instructions (10%; incubation of 4 h at 37 °C and 5% CO<sub>2</sub>). Metabolically active cells were able to reduce the dye, and the fluorescence generated was quantified using a microplate reader

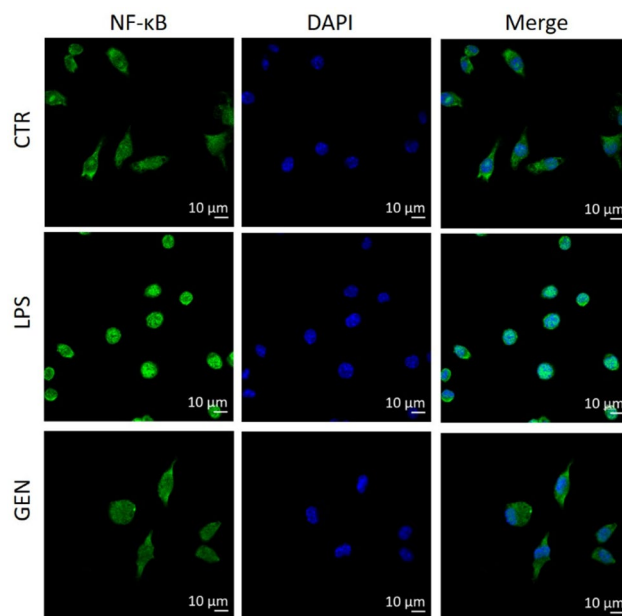


**Fig. 7.** NF- $\kappa$ B p65 nuclear translocation in LPS-stimulated macrophages treated with genistein. J774 macrophages were not treated with LPS in CTR samples (upper row), treated with LPS alone for 30 min (middle row), or pre-treated with genistein (5  $\mu$ g/mL) for 4 h and then LPS-stimulated for 30 min (bottom row). NF- $\kappa$ B p65 is stained with Alexa Fluor<sup>®</sup> 488 (green) while nuclei are stained with DAPI (blue). Data are represented as mean  $\pm$  SD obtained from at least three independent biological experiments, performed in triplicate.

(Varioskan Lux, Thermo Fisher, Waltham, MA, USA) with 530/590 nm excitation/emission wavelengths. Results were expressed as viability percentage normalized over the control samples (non-treated cells, 100% viability).

#### Analysis of cell cycle and DNA content

The effect of genistein on J774 cell cycle was analysed using the PI/RNase Solution Kit (Immunostep, Salamanca, Spain). Briefly, cells were seeded at a density of  $2 \times 10^4$  cells/cm<sup>2</sup> in 60 mm dishes and treated with 5  $\mu$ g/mL genistein. After 24 h of incubation, cells were harvested, fixed in 70% ice-cold ethanol and stored at 4°C for 24 h. Samples were then centrifuged ( $413 \times g$ , 5 min), rehydrated in PBS and stained with propidium iodide (PI) solution (50  $\mu$ g/mL) containing RNase A (100  $\mu$ g/mL). PI-stained cells were analyzed for DNA content by flow cytometry using a Beckman Coulter Gallios cytometer (Brea, CA, USA).

#### Evaluation of cell apoptosis

Cells were seeded at a density of  $2 \times 10^4$  cells/cm<sup>2</sup> in 60 mm dishes and treated with 5  $\mu$ g/mL genistein for 24 h. After the incubation period, cells were collected, washed in PBS, centrifuged (1500 rpm, 5 min) and resuspended in annexin V-binding buffer (10 mM HEPES/NaOH pH 7.4, 140 mM NaCl, 2.5 mM CaCl<sub>2</sub>). Then, 5  $\mu$ L of Annexin V-FITC and 5  $\mu$ L of propidium iodide were added to each tube. Cells were incubated at room temperature for 15 min in the dark and 400  $\mu$ L of annexin binding buffer was added. The signal intensity was measured by flow cytometry using a Beckman Coulter Gallios (Brea, CA, USA). A negative control with untreated cells was used to define the basal level of apoptotic and necrotic or dead cells.

#### Mitochondrial membrane potential assay

J774 cells were seeded in 60 mm dishes and treated with 5  $\mu$ g/mL genistein for 24 h, using cells not treated with genistein as control. After treatment, cells were washed twice, resuspended in PBS, and 5  $\mu$ L of 10  $\mu$ M 1,1',3,3,3'-hexamethylindodicarbo-cyanine iodide (DiIc1) were added to each sample. Samples were incubated at 37 °C for 15 min following addition of 400  $\mu$ L of PBS prior to the analysis of fluorescence with a Beckman Coulter Gallios flow cytometer (Brea, CA, USA). Excitation and emission parameters were set at 633 nm and 658 nm, respectively. Results are expressed as a percentage of cells exhibiting altered mitochondrial potential.

#### Reactive oxygen species (ROS) production

To determine the intracellular level of ROS produced, the dichlorofluorescein assay was used. J774 cells were seeded at a density of  $2 \times 10^4$  cells/cm<sup>2</sup> in 96-well plates and incubated for 24 h under standard cell culture conditions, following treatment with 5  $\mu$ g/mL genistein for 24 h. Then, the medium was removed, cells were washed twice with PBS and incubated with 100  $\mu$ L of 10  $\mu$ M 2',7'-dichlorofluorescein diacetate (DCFH-DA) in cell culture medium at 37°C for 30 min. Some wells were incubated with 100  $\mu$ L of 80 mM H<sub>2</sub>O<sub>2</sub> to induce oxidative stress prior to DCFH-DA addition. The fluorescence produced by the formation of the oxidized

derivate of 2', 7' -dichlorofluorescein (CDF) was measured at 485 and 535 nm wavelengths, excitation and emission respectively, using a microplate reader (Varioskan Lux, Thermo Fisher, Waltham, MA, USA).

### Determination of proteasome activity

Cells ( $2 \times 10^4$  cells/well/90  $\mu$ L) were seeded in 96-well plates at 37 °C in supplemented medium, overnight. Proteasome activity determination involved a fluorometric assay utilizing the Proteasome 20 S Activity Kit (MAK172, Sigma-Aldrich). This assay employed LLVY-R110 as a fluorogenic indicator for proteasome activities. 10  $\mu$ L of genistein at a concentration of 5  $\mu$ g/mL were added to J774 cells for 24 h and the cells were analysed according to the manufacturer's instructions. The fluorescence measurements indicated the chymotrypsin-like activity of the proteasome (CT-L activity), with heightened fluorescence signifying increased proteasome 20 S activity.

### In vitro induction of inflammation and treatment in cell culture

Two different approaches were employed in the development of in vitro inflammation and treatment with genistein. On the one hand, the pre-treatment approach included a 30 min treatment with genistein 5  $\mu$ g/mL. Then, inflammation was induced by addition of 100 ng/mL of LPS for 24 h at 37 °C and 5% CO<sub>2</sub>, without removing the medium. On the other hand, for the post-treatment approach, J774 cells were stimulated with LPS 100 ng/mL for 3 h at 37 °C and 5% CO<sub>2</sub>. After the incubation, genistein 5  $\mu$ g/mL was added without discarding the medium containing LPS.

### Nitric oxide (NO) production

NO levels were determined through the Griess reaction, which enables the detection of nitrite, a stable metabolite of NO. For this purpose, J774 cells were seeded in 12-well plates at a density of  $6.2 \times 10^4$  cells/cm<sup>2</sup> and stimulated with LPS following the treatments described above. Then, 100  $\mu$ L of the cellular supernatant was mixed with 100  $\mu$ L of Griess reagent. The mixture was incubated for 15 min at room temperature, and absorbance was measured at 540 nm using a Varioskan Lux plate reader (Thermo Fisher, Waltham, MA, USA). The amount of nitrite in the samples was calculated based on a freshly prepared standard curve of sodium nitrite in cell culture medium (0.78–100  $\mu$ M).

### Gene expression analysis

Cells ( $2 \times 10^4$  cells/cm<sup>2</sup>) were seeded in 6-well plates and stimulated following the pre-treatment and post-treatment approaches explained above. Next, cells were collected to analyse their gene expression by real time quantitative polymerase chain reaction (RT-qPCR). For this purpose, cells were washed with PBS and lysed with TRIzol. RNA levels were assessed using the NanoDrop 2000 spectrophotometer (Thermo Fisher Scientific, Waltham, MA, USA). 500 ng of RNA were reverse transcribed to cDNA with PrimeScript™ RT Master Mix and PremixExTaq was used to carry out the DNA amplification, using a QuantStudio™ 5 Real-Time PCR Instrument (Applied Biosystems, Waltham, MA, USA) under the following conditions: 30 s at 95 °C, followed by 40 cycles of 5 s at 95 °C and 30 s at 60 °C. Gene expression was evaluated using the following target probes (Integrated DNA Technologies, Neward, NJ, USA):

- Pro-inflammatory genes: Nos2 (Mm.PT.58.43705194), IL-6 (Mm.PT.58.10005566), IL-1b (Mm.PT.58.41616450).
- Anti-inflammatory genes: TGF- $\beta$ 1 (Mm.PT.58.11254750).

Gene expression was normalized to the level of actin beta (Mm.PT.39a.22214843.g). Results were represented as a percentage of LPS, which was chosen as the reference at 100%. The  $2^{-\Delta\Delta CT}$  method was used to analyse the data. Samples were analysed in triplicates and represented as mean  $\pm$  SD.

### Western blot

J774 cells were seeded at a density of  $2 \times 10^4$  cells/cm<sup>2</sup> in 100 mm dishes, and stimulated with LPS following the pre-treatment and post-treatment approaches. Next, cells were washed with PBS and total protein was extracted and quantified using a BCA Protein Assay Kit (Thermo Fisher Scientific, Waltham, MA, USA). After, 75  $\mu$ g measured proteins were loaded and separated on 8% dodecyl sulphate sodium salt (SDS)-polyacrylamide gel electrophoresis, then transferred onto nitrocellulose membrane at 4 °C. After that, the membrane was blocked with 5% BSA for 1 h at 4 °C, and the membrane was then endowed with primary antibody against iNOS at 4 °C overnight, followed by mouse anti-rabbit IgG-HRP sc-2357-CM secondary antibody at room temperature for 1 h. Immobilon Crescendo Western HRP substrate was used to visualize protein levels with the ChemiDoc™ MP Imaging System (Bio-Rad, USA). GAPDH antibody was used as housekeeping control.

### Enzyme-linked immunosorbent assay (ELISA)

Cells ( $6.2 \times 10^4$  cells/cm<sup>2</sup>) were seeded in 12-well plates and stimulated with LPS following the treatments described above. After, the culture supernatant was collected for the measurement of TNF- $\alpha$  and IL-6 levels with ELISA kit (Thermo Fisher, Waltham, MA, USA), following the manufacturer's instructions.

### Analysis of cell morphology

J774 cells ( $6.2 \times 10^4$  cells/cm<sup>2</sup>) were seeded onto 24-well plates on glass coverslips and stimulated with LPS following the pre-treatment and post-treatment approaches described above. Next, cells were washed twice in PBS and fixed in 4% paraformaldehyde for 15 min at room temperature. Cells were washed thrice with PBS and stained with wheat germ agglutinin Alexa Fluor™ 488 Conjugate following manufacturer's instructions in order

to stain cell membrane. Finally, nuclei were stained with DAPI (Molecular Probes, Eugene, OR, USA) for 30 min in the dark and mounted using Mowiol mounting medium (Thermo Fisher, Waltham, MA, USA). Images were collected using a Leica TCS SP2 Laser Scanning Confocal Microscope (München, Germany).

### Evaluation of NF- $\kappa$ B translocation

Cells were cultured at a density of  $2 \times 10^4$  cells/cm<sup>2</sup> onto 24-well plates on glass coverslips and pre-treated with genistein 5  $\mu$ g/mL for 30 min prior to stimulation with LPS for another 30 min. Next, cells were fixed with cold formaldehyde (3.7% in PBS) for 15 min, washed with PBS and incubated for 1 h with blocking buffer (containing 5% normal goat serum (Sigma-Aldrich, St. Louis, MO, USA) and 0.3% Triton X-100 (Sigma-Aldrich, St. Louis, MO, USA) at room temperature. After, cells were first stained with anti-NF- $\kappa$ B/p65 rabbit monoclonal antibody (1:100; Abcam, Cambridge, UK) and later incubated with a secondary Alexa Fluor<sup>®</sup> 488 goat anti-rabbit IgG (H+L) polyclonal antibody (1:1000; Molecular Probes, Eugene, OR, USA). The nuclei was stained with 2  $\mu$ g/mL of DAPI (Molecular Probes, Eugene, OR, USA). Samples were mounted using Mowiol mounting medium (Thermo Fisher, Waltham, MA, USA). Images were collected using a Leica TCS SP2 Laser Scanning Confocal Microscope (München, Germany).

### Statistical analysis

Statistical analysis of the data was performed using GraphPad version 8 software (GraphPad Software, Inc. La Jolla, CA, USA). A one-way analysis of variance (ANOVA) set was used for multiple comparisons with a Tukey's post-test and an unpaired t-test. All experiments were performed using at least three independent biological replicates, each containing three technical replicates. Data are presented as mean  $\pm$  SD.

### Conclusion

Macrophages play a pivotal role in the release of inflammation mediators being essential in complex physiological and pathological processes such as acute and chronic inflammation, immunity and tissue regeneration. The development of novel therapeutic strategies, based in personalized and precision medicine for the modulation of macrophages polarization and function, makes imperative the deep understanding of cellular and molecular events in macrophages. The use of natural biologically active compounds such as flavonoids and, specifically, genistein, would involve a promising tool to achieve the regulation of macrophages and the modification of their polarization state. Our work reveals the effectiveness of genistein in the regulation of macrophage phenotype and M1/M2 ratio and therefore, in inflammation. The treatment of J774 macrophages with genistein did not involve cell apoptosis or cell cycle arrest, also providing the regulation of cell oxidative status while preserving cell viability. Moreover, the induction of inflammation by means of LPS following the pre- and post-treatment strategies highlighted the beneficial effects of genistein in the depletion of the expression of proinflammatory markers while increasing the expression of the anti-inflammatory ones. Cell morphology and size as well as the disruption in the nuclear translocation of NF- $\kappa$ B p65 subunit were also reverted to the basal state of control cells after genistein treatment. Our results confirm the anti-inflammatory capacity and the potential reversion of macrophages polarization mediated by genistein treatment at both gene and protein levels. Ongoing research regarding the targeting of macrophages would involve great advances in the improvement of inflammation therapies. Nevertheless, the translation of in vitro findings to clinical applications remains challenging due to differences in bioavailability, metabolism and the complexity of in vivo inflammatory environments. Further studies in animal models and human systems are required to validate the therapeutic potential of genistein.

### Data availability

Data will be made available from the corresponding author on reasonable request.

Received: 24 October 2025; Accepted: 25 February 2026

Published online: 02 March 2026

### References

- Chavda, V. P., Feehan, J. & Apostolopoulos, V. Inflammation: The Cause of All Diseases. *Cells* **13**, 1906 (2024).
- Lawrence, T. The nuclear factor NF- $\kappa$ B pathway in inflammation. *Cold Spring Harb Perspect. Biol.* **1**, a001651 (2009).
- Chen, L. Inflammatory responses and inflammation-associated diseases in organs. *Oncotarget* **9**, 7204–7218 (2018).
- Zhang, S. et al. Mechanisms of Baicalin Alleviates Intestinal Inflammation: Role of M1 Macrophage Polarization and Lactobacillus amylovorus. *Adv. Sci.* **12**, e2415948 (2025).
- Zhu, X. et al. The Role of T Cells and Macrophages in Asthma Pathogenesis: A New Perspective on Mutual Crosstalk. *Mediators Inflamm.* 7835284. (2020).
- Gan, Z., Zhao, M., Xia, Y., Yan, Y. & Ren, W. Carbon metabolism in the regulation of macrophage functions. *Trends Endocrinol. Metab.* **35**, 65–73 (2024).
- Siebeler, R., de Winther, M. P. J. & Hoeksema, M. A. The regulatory landscape of macrophage interferon signaling in inflammation. *J. Allergy Clin. Immunol.* **152**, 326–337 (2023).
- Yunna, C., Mengru, H., Lei, W. & Weidong, C. Macrophage M1/M2 polarization. *Eur. J. Pharmacol.* **877**, 173090 (2020).
- Van Dyken, S. J. & Locksley, R. M. Interleukin-4- and interleukin-13-mediated alternatively activated macrophages: roles in homeostasis and disease. *Annu. Rev. Immunol.* **31**, 317–343 (2013).
- Zhang, J., Cianciosi, D., Islam, M. O., Zhang, L. & Editorial Intervention effects of food-derived polyphenols and bioactive peptides on chronic inflammation. *Front. Nutr.* **11**, 1493706 (2024).
- Skrainowska, D., Szterk, A., Ofiara, K., Kowalczyk, P. & Bobrowska-Korczak, B. The Genistein Supply and Elemental Composition of Rat Kidneys in an Induced Breast Cancer Model. *Nutrients* **17**, 1184 (2025).
- Yang, W. et al. An exhaustive examination of the research progress in identifying potential JAK inhibitors from natural products: a comprehensive overview. *Chin. Med.* **20**, 130 (2025).

13. Kattna, A. & Singh, L. Genistein as a renoprotective agent: mechanistic insights into antioxidant, anti-inflammatory, and fibrosis-regulating pathways. *Mol. Biol. Rep.* **52**, 500 (2025).
14. Bansal, K., Singh, V., Mishra, S. & Bajpai, M. Articulating the Pharmacological and Nanotechnological Aspects of Genistein: Current and Future Prospectives. *Curr. Pharm. Biotechnol.* **25**, 807–824 (2024).
15. Abron, J. D. et al. Genistein induces macrophage polarization and systemic cytokine to ameliorate experimental colitis. *PLoS One*. **13**, e0199631 (2018).
16. Quan, S. et al. Genistein Promotes M2 Macrophage Polarization via Aryl Hydrocarbon Receptor and Alleviates Intestinal Inflammation in Broilers with Necrotic Enteritis. *Int. J. Mol. Sci.* **25**, 6656 (2024).
17. Ji, G. et al. Genistein suppresses LPS-induced inflammatory response through inhibiting NF- $\kappa$ B following AMP kinase activation in RAW 264.7 macrophages. *PLoS One*. **7**, e53101 (2012).
18. Li, Y. et al. Exploring the anti-aging potential of phytoestrogens: focus on molecular mechanisms and menopausal symptom modulation. *Front. Nutr.* **12**, 1651367 (2025).
19. Zhang, K., Wang, J. & Xu, B. Critical Review on Molecular Mechanisms for Genistein's Beneficial Effects on Health Through Oxidative Stress Reduction. *Antioxid. (Basel)*. **14**, 904 (2025).
20. Singh, P. & Paramanik, V. DNA methylation, histone acetylation in the regulation of memory and its modulation during aging. *Front. Aging*. **5**, 1480932 (2025).
21. Standard, I. Part 5: tests for in vitro cytotoxicity tanzania bureau of standards. *Biol. Eval. Med. Dev.* **9**, (2009).
22. Bitto et al. The steady-state serum concentration of genistein aglycone is affected by formulation: a bioequivalence study of bone products. *BioMed Res. Int.* 273498 (2013). (2013).
23. van der Velpen, V. et al. Large inter-individual variation in isoflavone plasma concentration limits use of isoflavone intake data for risk assessment. *Eur. J. Clin. Nutr.* **68**, 1141–1147 (2014).
24. Mathey, J. et al. Concentrations of isoflavones in plasma and urine of post-menopausal women chronically ingesting high quantities of soy isoflavones. *J. Pharm. Biomed. Anal.* **41**, 957–965 (2006).
25. Cui, S., Wienhoefer, N. & Bilitewski, U. Genistein induces morphology change and G2/M cell cycle arrest by inducing p38 MAPK activation in macrophages. *Int. Immunopharmacol.* **18**, 142–150 (2014).
26. Goh, Y. X. et al. A Review on its Anti-Inflammatory Properties. *Front. Pharmacol.* **13**, 820969 (2022).
27. Hsieh, H. M., Wu, W. M. & Hu, M. L. Genistein Attenuates D-Galactose-Induced Oxidative Damage through Decreased Reactive Oxygen Species and NF- $\kappa$ B Binding Activity in Neuronal PC12 Cells. *Life Sci.* **88**, 82–88 (2011).
28. Han, S., Wu, H., Li, W. & Gao, P. Protective Effects of Genistein in Homocysteine-Induced Endothelial Cell Inflammatory Injury. *Mol. Cel Biochem.* **403**, 43–49 (2015).
29. Bhattarai, G., Poudel, S. B., Kook, S. H. & Lee, J. C. Anti-inflammatory, Anti-osteoclastic, and Antioxidant Activities of Genistein Protect against Alveolar Bone Loss and Periodontal Tissue Degradation in a Mouse Model of Periodontitis. *J. Biomed. Mater. Res. A*. **105**, 2510–2521 (2017).
30. Smolińska, E. et al. Molecular Action of Isoflavone Genistein in the Human Epithelial Cell Line HaCaT. *PLoS ONE*. **13**, e0192297 (2018).
31. Liu, F. C. et al. Chondroprotective Effects of Genistein against Osteoarthritis Induced Joint Inflammation. *Nutrients* **11**, 1180 (2019).
32. Paesa, M. et al. Valorization of Onion Waste by Obtaining Extracts Rich in Phenolic Compounds and Feasibility of Its Therapeutic Use on Colon Cancer. *Antioxid. (Basel)*. **11**, 733 (2022).
33. Kamińska, J. et al. The preliminary study suggests an association between NF- $\kappa$ B pathway activation and increased plasma 20S proteasome activity in intracranial aneurysm patients. *Sci. Rep.* **14**, 3941 (2024).
34. Alorda-Clara, M. et al. High Concentrations of Genistein Decrease Cell Viability Depending on Oxidative Stress and Inflammation in Colon Cancer Cell Lines. *Int. J. Mol. Sci.* **23**, 7526 (2022).
35. Pagliacci, M. C. et al. Genistein inhibits tumour cell growth in vitro but enhances mitochondrial reduction of tetrazolium salts: a further pitfall in the use of the MTT assay for evaluating cell growth and survival. *Eur. J. Cancer.* **29A**, 1573–1577 (1993).
36. Choi, C., Cho, H., Park, J., Cho, C. & Song, Y. Suppressive effects of genistein on oxidative stress and NF $\kappa$ B activation in RAW 264.7 macrophages. *Biosci. Biotechnol. Biochem.* **67**, 1916–1922 (2003).
37. Choi, E. Y. et al. Genistein suppresses Prevotella intermedia lipopolysaccharide-induced inflammatory response in macrophages and attenuates alveolar bone loss in ligature-induced periodontitis. *Arch. Oral Biol.* **62**, 70–79 (2016).
38. Sheu, F., Lai, H. H. & Yen, G. C. Suppression effect of soy isoflavones on nitric oxide production in RAW 264.7 macrophages. *J. Agric. Food Chem.* **49**, 1767–1772 (2001).
39. Akaraseneont, P., Mitchell, J. A., Appleton, I., Thiemermann, C. & Vane, J. R. Involvement of tyrosine kinase in the induction of cyclo-oxygenase and nitric oxide synthase by endotoxin in cultured cells. *Br. J. Pharmacol.* **113**, 1522–1528 (1994).
40. Hämäläinen, M., Nieminen, R., Vuorela, P., Heinonen, M. & Moilanen, E. Anti-inflammatory effects of flavonoids: genistein, kaempferol, quercetin, and daidzein inhibit STAT-1 and NF- $\kappa$ B activations, whereas flavone, isorhamnetin, naringenin, and pelargonidin inhibit only NF- $\kappa$ B activation along with their inhibitory effect on iNOS expression and NO production in activated macrophages. *Mediators Inflamm.* 45673 (2007).
41. Pulendran, B., Palucka, K. & Banchereau, J. Sensing pathogens and tuning immune responses. *Science* **293**, 253–256 (2001).
42. Caroff, M., Karibian, D. & Cavaillon, J. M. Haeflner-Cavaillon, N. Structural and functional analyses of bacterial lipopolysaccharides. *Microbes Infect.* **4**, 915–926 (2002).
43. Jeong, J. W. et al. Anti-inflammatory effects of genistein via suppression of the toll-like receptor 4-mediated signaling pathway in lipopolysaccharide-stimulated BV2 microglia. *Chem. Biol. Interact.* **212**, 30–39 (2014).
44. Kim, D. H. et al. Genistein Inhibits Pro-inflammatory Cytokines in H-uman M-ast C-ell A-ctivation through the I-nhibition of the ERK P-athway. *Int. J. Mol. Med.* **34**, 1669–1674 (2014).
45. García-Salinas, S. et al. Electrospun anti-inflammatory patch loaded with essential oils for wound healing. *Int. J. Pharm.* **577**, 119067 (2020).
46. Ganai, A. A., Khan, A. A., Malik, Z. A. & Farooqi, H. Genistein modulates the expression of NF- $\kappa$ B and MAPK (p-38 and ERK1/2), thereby attenuating d-Galactosamine induced fulminant hepatic failure in Wistar rats. *Toxicol. Appl. Pharm.* **283**, 139–146 (2015).
47. Tang, H. et al. Prospects of and limitations to the clinical applications of genistein. *Discov Med.* **27**, 177–188 (2019).

## Acknowledgements

C.R. acknowledge the support from Regional Government of Aragon (Orden CUS/803/2021) while G.M. acknowledges the support from the Miguel Servet Program (MS19/00092; Instituto de Salud Carlos III).

## Author contributions

C.R: Data curation, Formal analysis, Investigation, Methodology, Software, Writing-original draft; S.L: Data curation, Investigation, Methodology, Writing-review and editing; G.M: Conceptualization, Formal analysis, Funding acquisition, Supervision, Validation, Writing-original draft.

## Funding

This research was funded by Instituto de Salud Carlos III (ISCIII, Spain; grant number PI21/00911 and “PROGRAMA FORTALECE DEL MINISTERIO DE CIENCIA E INNOVACIÓN” grant number FORT23/00028), Department of Employment, Science and Universities of Regional Government of Aragon (grant number PROY\_B55\_24), and Aragon Health Research Institute (IIS Aragon, Spain; grant number INTRAMURAL23/GE).

## Declarations

### Competing interests

The authors declare no competing interests.

### Additional information

**Supplementary Information** The online version contains supplementary material available at <https://doi.org/10.1038/s41598-026-42357-7>.

**Correspondence** and requests for materials should be addressed to C.R.G.

**Reprints and permissions information** is available at [www.nature.com/reprints](http://www.nature.com/reprints).

**Publisher’s note** Springer Nature remains neutral with regard to jurisdictional claims in published maps and institutional affiliations.

**Open Access** This article is licensed under a Creative Commons Attribution-NonCommercial-NoDerivatives 4.0 International License, which permits any non-commercial use, sharing, distribution and reproduction in any medium or format, as long as you give appropriate credit to the original author(s) and the source, provide a link to the Creative Commons licence, and indicate if you modified the licensed material. You do not have permission under this licence to share adapted material derived from this article or parts of it. The images or other third party material in this article are included in the article’s Creative Commons licence, unless indicated otherwise in a credit line to the material. If material is not included in the article’s Creative Commons licence and your intended use is not permitted by statutory regulation or exceeds the permitted use, you will need to obtain permission directly from the copyright holder. To view a copy of this licence, visit <http://creativecommons.org/licenses/by-nc-nd/4.0/>.

© The Author(s) 2026